


Oleylethanolamide Increases Glycogen Synthesis and Inhibits Hepatic Gluconeogenesis via the LKB1/AMPK Pathway in Type 2 Diabetic Model^{SI}

Tong Ren, Ang Ma, Rengong Zhuo, Huaying Zhang, Lu Peng, Xin Jin, Enhui Yao, and  Lichao Yang

Xiamen Key Laboratory of Chiral Drugs, School of Medicine, Xiamen University, Xiamen, China (T.R., A.M., R.Z., H.Z., L.P., X.J., L.Y.) and Department of Cardiology, Fujian Medical University Union Hospital, Fujian Institute of Coronary Artery Disease, Fujian Heart Medical Center, Fuzhou, China (E.Y.)

Received September 13, 2019; accepted January 7, 2020

ABSTRACT

Oleylethanolamide (OEA) is an endogenous peroxisome proliferator-activated receptor α (PPAR α) agonist that acts on the peripheral control of energy metabolism. However, its therapeutic potential and related mechanisms in hepatic glucose metabolism under type 2 diabetes mellitus (T2DM) are not clear. Here, OEA treatment markedly improved glucose homeostasis in a PPAR α -independent manner. OEA efficiently promoted glycogen synthesis and suppressed gluconeogenesis in mouse primary hepatocytes and liver tissue. OEA enhanced hepatic glycogen synthesis and inhibited gluconeogenesis via liver kinase B1 (LKB1)/5' AMP-activated protein kinase (AMPK) signaling pathways. PPAR α was not involved in the roles of OEA in the LKB1/AMPK pathways. We found that OEA exerts its antidiabetic effect by

increasing glycogenesis and decreasing gluconeogenesis via the LKB1/AMPK pathway. The ability of OEA to control hepatic LKB1/AMPK pathways may serve as a novel therapeutic approach for the treatment of T2DM.

SIGNIFICANCE STATEMENT

Oleylethanolamide (OEA) exerted a potent antihyperglycemic effect in a peroxisome proliferator-activated receptor α -independent manner. OEA played an antihyperglycemic role primarily via regulation of hepatic glycogen synthesis and gluconeogenesis. The main molecular mechanism of OEA in regulating liver glycometabolism is activating the liver kinase B1/5' AMP-activated protein kinase signaling pathways.

Introduction

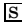
Type 2 diabetes mellitus (T2DM) is characterized by disrupted glucose homeostasis largely due to insulin resistance (IR) in target tissue (Danaei et al., 2011). The liver is the main site for glycogen storage and the trigger for circulating glucose flow (Nordlie et al., 1999). Glycogen synthesis improves glucose uptake and storage under physiologic conditions (Nordlie et al., 1999; Moore et al., 2018). However, liver sensitivity to insulin is reduced during IR, and hepatic glycogen synthesis declines, which results in the inefficient conversion of circulating glucose (von Wilamowitz-Moellendorff et al., 2013). Another major

reason for hyperglycemia is increased hepatic glucose production via aberrantly activated gluconeogenesis in insulin-resistant liver (Miller et al., 2013). Therefore, hepatic gluconeogenesis inhibitors are used as first-line antidiabetes drugs, that is, metformin and pioglitazone, which always work as an effective therapeutic approach for T2DM (Foretz et al., 2010; Duca et al., 2015; He et al., 2016; Petersen et al., 2017). Adipose is another initial peripheral insulin-resistant tissue. IR in the liver is a more sensitive factor than adipose tissue as a cause for fasting hyperglycemia and T2DM (Grundy, 2015; Dong et al., 2016). Increased glucose production and reduced hepatic glycogen storage are the two most prominent features that contribute to metabolic abnormalities in diabetes (Haeusler et al., 2014).

Oleylethanolamide (OEA) is an endocannabinoid that is produced by circadian enterocytes (Brown et al., 2017). Its administration plays an important role in dyslipidemia regulation by enhancing fatty acid β/ω -oxidation, prolonging eating latency or reducing meal size via peroxisome proliferator-activated receptor α (PPAR α) activation in the

This study was supported by grants from the National Natural Sciences Foundation of China (81973306, 81872866, and 81601227), the Fundamental Research Funds for the Central Universities (20720180042), the Health Science Research Personnel Training Program of Fujian Province (2018-CXB-30), and the Natural Science Foundation of Fujian, China (2016J01415 and 2016D019).

<https://doi.org/10.1124/jpet.119.262675>.

 This article has supplemental material available at jpet.aspetjournals.org.

ABBREVIATIONS: AMPK, 5'-AMP-activated protein kinase; DM, diabetes mellitus; DMEM, Dulbecco's modified Eagle's medium; G6Pase, glucose 6-phosphatase; GPR, G protein-coupled receptor; GSK, glycogen synthase kinase; HFD, high-fat diet; HOMA-IR, homeostatic model assessment of IR; IR, insulin resistance; KO, knockout; LDL-C, low-density lipoprotein cholesterol; LKB1, liver kinase B1; NAAA, *N*-acylethanolamine acid amidase; OEA, oleylethanolamide; PA, palmitic acid; PAS, periodic acid-Schiff; PEPCK, phosphoenolpyruvate carboxykinase; PPAR α , peroxisome proliferator-activated receptor α ; SD, Sprague-Dawley; STZ, streptozotocin; T2DM, type 2 DM; TC, total cholesterol; TG, triglyceride p-GSK-3 β phosphorylation-GSK-3 β , p-AMPK- α Thr172 phosphorylation-AMPK- α Thr172, p-LKB1 phosphorylation-LKB1 siRNA Small interference RNA CB1 cannabinoid receptor 1.

liver tissue and proximal small intestine (Fu et al., 2003; Brown et al., 2017). OEA stimulates lipolysis in adipocytes because it increases the release of nonesterified fatty acids and glycerol in a PPAR α -mediated manner (Guzmán et al., 2004; Gaetani et al., 2008). Serum OEA levels are markedly increased in T2DM mammals (Annuzzi et al., 2010). The role of OEA in G protein-coupled receptor (GPR) 119 and GPR55 activation suggests that it regulates insulin secretion in pancreatic islet cells (McKillop et al., 2013). OEA is hydrolyzed to release free oleate, which regulates cytoprotection in β -cells (Stone et al., 2012). Previous studies of OEA in glucose metabolism balance primarily focused on adipocytes and β -cells (González-Yanes et al., 2005; Martínez de Ubago et al., 2009). In addition, the liver is a main target organ for the regulation of glucose metabolism via regulating gluconeogenesis and glycogen synthesis. Furthermore, our latest study indicates that OEA exerted antidiabetic effects in high-fat diet (HFD) and streptozotocin (STZ)-induced mice (Ren et al., 2019). However, it is unclear whether OEA inhibits the elevation of blood sugar by regulating hepatic gluconeogenesis and glycogen synthesis.

Hepatocytes express more PPAR α than adipocytes. Our previous study showed that OEA ameliorated diabetes-induced cognitive deficits via a PPAR α -mediated pathway (Ren et al., 2019). Whether PPAR α is a key target for the effect of OEA on hepatocyte glucose metabolism balance is not clear. In the present study, we used Sprague-Dawley (SD) rats, 129S4/SvJae mice, and PPAR α knockout mice subjected to HFD/STZ-induced T2DM model or palmitic acid (PA)-stimulated mouse primary hepatocytes to investigate the effect of OEA on glucose homeostasis, especially hepatic glycogen synthesis and gluconeogenesis. Furthermore, we examined the underlying mechanism of OEA in regulating hepatic glycogen synthesis and gluconeogenesis.

Methods and Experimental Procedures

Animal Preparations. Male SD rats (6–8 weeks old, weighing 160–170 g, male) were purchased from Vital River Laboratory Animal Technology Co. Ltd. (Beijing, China). The 129S4/SvJae mice (7–9 weeks old, male) and PPAR α knockout mice (129S4/SvJae-Pparatm1Gonz/J) (7–9 weeks old, male) weighing 20–22 g were purchased from Jackson Laboratory (Bar Harbor, ME). All animals were maintained in specific pathogen-free conditions in a 12-hour light/dark cycle environment with unrestricted access to food and water. All animal studies (including mouse euthanasia procedures) were performed in compliance with the institutional animal care regulations and guidelines of Xiamen University and according to the Animal Research: Reporting of In Vivo Experiments and Institutional Animal Care and Use Committee guidelines. Maximum efforts were made to minimize the pain and suffering of the animals.

HFD and STZ-Induced Model of T2DM. Animals were fed a lard oil and sucrose-enriched HFD for 6 weeks. An intraperitoneal injection of STZ (35 mg/kg for rats or 40 mg/kg for mice) was administered the day after placement on the HFD. The HFD incorporated 30% fat, 20% sugar, 15% protein, 2.5% cholesterol, 1% sodium cholic acid, and 31.5% custom carbohydrate (Gilbert et al., 2011; Xu et al., 2015).

Treatment. Animals received a single daily intraperitoneal injection of OEA (10, 30, or 60 mg/kg dissolved in Tween 20/saline, 10/90) or vehicle (saline, 10% Tween 20) for 6 weeks. The schedule is shown in Supplemental Fig. 1.

Measurement of Metabolites. We measured fasting blood glucose levels using a blood glucose meter (Johnson & Johnson, New Brunswick). We measured plasma insulin levels using an ELISA kit (ALPCO, Windham, NH). Insulin resistance was assessed via calculating the homeostatic model assessment of insulin resistance (HOMA-IR), which was previously described. The serum concentrations of total cholesterol (TC), triglyceride (TG), low-density lipoprotein cholesterol (LDL-C), and glycogen levels were measured using commercial assay kits (Jiancheng, China) according to the manufacturer's instructions.

Periodic Acid-Schiff Staining. Immediately following termination of the experiments, the liver tissue was fixed with 4% paraformaldehyde after removal from anesthetized rats. The tissue was embedded in optimal cutting temperature and sectioned into 6-mm slices. Hepatic glycogen was stained using periodic acid-Schiff (PAS) using commercial assay kits (Solarbio, Beijing, China) according to the manufacturer's protocol. Purple-stained parts indicate the presence of glycogen, and these parts were examined using a light microscope.

Western Blot Analysis. Protein extracts were electrophoresed, blotted, and incubated with the following primary antibodies (1:1000) at 4°C overnight: anti-glycogen synthase kinase (GSK)-3 β (Cell Signaling Technology); anti-pGSK3 β Ser9 (Cell Signaling Technology); anti-phosphoenolpyruvate carboxykinase (PEPCK) (Abcam); anti-glucose 6-phosphatase (G6pase) (Abcam); anti-AMPK (Cell Signaling Technology); anti-pAMPK- α Thr172 (Cell Signaling Technology); anti-liver kinase B1 (LKB1) (Cell Signaling Technology); anti-pLKB1 Ser428 (Cell Signaling Technology), and β -actin (1:10,000; Abcam). The membranes were washed three times with Tris-buffered saline/Tween 20 and incubated with the appropriate secondary horseradish peroxidase-conjugated antibodies (diluted 1:10,000 in 5% skim milk) at room temperature for 1 hour. The membranes were washed in Tris-buffered saline/Tween 20 five times for 5 minutes each, and the protein bands were visualized and quantified using scanning densitometry in ImageStation 4000R (Rochester, NY).

Cell Culture. Primary mouse hepatocytes were isolated from male C57/BL6 mice according to a previously reported method and cultured at 37°C in a 5% humidified CO₂ incubator. After the cells adhered to the plate, the medium was changed to Dulbecco's modified Eagle's medium (DMEM) supplemented with 1000 mg/l glucose and 0.3 mM PA (Sigma) and incubated for 24 hours to establish insulin resistance (Liu et al., 2015). The cells were treated the following day with saline or OEA (20 or 40 μ M; Sigma-Aldrich) for 0, 6, 12, 24, or 36 hours. The cells were seeded in six-well plates, and then GPR119 agonist PSN632408 (20 μ M) and AMPK agonist metformin (20 μ M) were dissolved into the medium before administration of OEA according to the manufacturer's instructions (MCE). Cells were lysed in radioimmunoprecipitation assay lysis buffer (Solarbio) containing a protease inhibitor mixture (Roche Applied Science), and protein concentrations were determined using the BCA protein assay (Thermo Scientific).

Bioinformatic Analysis. T2DM gene expression data were obtained from the Gene Expression Omnibus database (<http://www.ncbi.nlm.nih.gov/geo>). Datasets from GSE13760 were included in this study. Raw CEL files were downloaded from the Gene Expression Omnibus database and normalized using Robust Multichip Average. Blast+2.2.30 was used to reannotate probes on GENCODE Release 21 sequence databases

for mRNA. For multiple probes corresponding to one gene, the maximum normalized signal was selected to generate the expression of mRNA. Two-sample *t* test or paired-sample *t* test was used according to the experimental design as a differential expression calling method, and then this was followed by Benjamini and Hochberg (false discovery rate) adjustment. To verify the expression correlation between genes, Pearson's correlation analysis was used after the CEL files were downloaded from GSE13760 and normalized by Robust Multichip Average (Assmann et al., 2017).

RNA Interference and Target Inhibitor. Primary mouse hepatocytes were seeded in six-well plates and transfected the next day with AMPK siRNA (100 nM), GPR119 siRNA (100 nM), or control siRNA (100 nM) using Lipofectamine 2000 (Invitrogen). AMPK siRNA (CTGCCAGAATTC CATTTA) and GPR119 siRNA (CTCTTTGTCTTCTTCTACT) were obtained from RIBOBIO. Transfected cells were harvested for further analyses. The LKB1 inhibitor Pim1/AKK1-IN-1 (Bamborough et al., 2008) (eBiochemicals) (20 μ M) was dissolved in the medium 6 hours before OEA administration according to the manufacturer's instructions (MCE).

Glucose Production Assay. The cells were treated with various concentrations of OEA in FBS and glucose-free DMEM for glucose production testing. The blank, normal (PA-free) cells and PA group cells were treated with the same bovine serum albumin DMEM for the same time duration. Glucose concentrations in the media were determined using a glucose oxidase-peroxidase assay kit (Nanjing Jiancheng Bioengineering Institute, China) after a 12-hour incubation. The levels of glucose production were normalized to the total protein content of whole-cell extracts.

OEA Biodistribution In Vivo. As we previously described (Yang et al., 2019), OEA at dose of 30 or 60 mg/kg was injected into peritoneal cavity of C57BL/6 mice. At 1, 5, 10, 20, 30, 60, 120, 240, and 360 minutes postinjection, the mice were sacrificed, and the liver was excised, which was followed by a washing of the surface with 0.9% NaCl for fluorescence intensity measurement (Cambridge Research & Instrumentation).

Pharmacokinetic Studies. OEA was dissolved in Tween-20/saline (10/90, v/v) and was administered to rats (30 or 60 mg/kg i.p.). After administrations, we anesthetized rats with halothane and collected blood at various time points (1, 5, 10, 20, 30, 60, 120, 240, and 360 minutes). Freshly extracted blood was collected and centrifuged immediately for 10 minutes at 3000 rpm in a refrigerated centrifuge (4°C). Plasma was then immediately separated from the blood and distributed in aliquots for further processing or stored at -80°C. Plasma samples were thawed in fewer than 30 minutes at room temperature and processed on ice. Aliquots of 0.25 ml were transferred into glass borosilicate tubes, diluted up to 0.5 ml with 0.1 M Ammonium acetate buffer (pH 4.0), extracted with 6 ml of tert-butyl methyl ether, and centrifuged (3500 rpm, 5 minutes) at room temperature. The organic phase was transferred to clean tubes and evaporated (40°C, 20 minutes) under a stream of nitrogen, and extracts were reconstituted in 100 μ l of a mixture of acetonitrile and transferred to high-pressure liquid chromatography vials. Twenty microliters were injected into the liquid chromatography with tandem mass spectrometry system. Liquid chromatography with tandem mass spectrometry analysis was according to previous protocol (Pastor et al., 2014).

Statistical Analysis. The results are expressed as the mean \pm S.E.M. Data for fasting blood glucose were compared

using two-way ANOVA followed by Bonferroni's post hoc test, and another statistical analysis was performed using one-way ANOVA with Tukey's post hoc test for comparisons between two groups (Prism 7 for Windows; GraphPad Software Inc.). Significance levels were established at a level of $P < 0.05$.

Results

OEA Ameliorated the HFD/STZ-Induced Hyperglycemia in a PPAR α -Independent Manner. Our latest study indicated that OEA inhibited the elevation of plasma glucose in HFD/STZ-induced mice (Ren et al., 2019). To further confirm the antidiabetic effects of OEA in vivo, HFD/STZ diabetic rats were administered OEA for 6 weeks. Consistent with the effect of OEA on suppressing plasma glucose in HFD/STZ-induced mice (Ren et al., 2019), OEA treatment dose-dependently decreased plasma glucose concentrations after 8-hour fasting in diabetic rats (Fig. 1A). Furthermore, OEA decreased insulin and HOMA-IR levels in diabetic rats, which exhibits its long-term impact on IR (Fig. 1, B and C). Additionally, OEA treatment markedly attenuated TC, TG, and LDL-C levels in HFD/STZ diabetic rats (Fig. 1D).

To evaluate the role of PPAR α in the hypoglycemic effect of OEA, diabetes mellitus (DM) was induced in PPAR α KO mice after 6 weeks of HFD and a single dose of STZ. Fasting plasma glucose concentrations increased significantly in wild-type mice (Sv129) and PPAR α KO mice after HFD/STZ treatment (Fig. 1E), which suggests that PPAR α was not a necessary factor in the pathologic development of hyperglycemia. However, OEA reduced the HFD/STZ-induced up-regulation of fasting blood glucose levels in wild-type and PPAR α KO mice (Fig. 1E). The level of HOMA-IR also decreased after OEA treatment in diabetic PPAR α KO mice (Fig. 1G). Therefore, OEA ameliorated the HFD/STZ-induced hyperglycemia in a PPAR α -independent manner. However, OEA had no effect on reducing serum levels of TC, TG, or LDL-C in diabetic PPAR α KO mice (Supplemental Fig. 2), which indicates that OEA amelioration of plasma lipid abnormalities in diabetic mice depended on PPAR α .

OEA Metabolism in Serum and Distribution in Liver. Given that OEA ameliorated the HFD/STZ-induced hyperglycemia at the doses of 30 and 60 mg/kg, we further examined the distribution of OEA in liver and plasma following intraperitoneal administration in rats. As shown in Supplemental Fig. 3, OEA (60 mg/kg i.p.) reached maximal plasma levels (C_{\max}) 10 minutes after injection and was slowly cleared from the circulation (Supplemental Fig. 3B). Its C_{\max} in plasma was 2-fold higher than that of OEA (30 mg/kg i.p.), indicating that OEA administration was, as expected, dose proportional.

OEA Enhanced Hepatic Glycogen Synthesis and Inhibited Gluconeogenesis during IR. Based on the glucose metabolism pathway, we focused on the ability of OEA to regulate hepatic glycogen and gluconeogenesis in HFD/STZ diabetic rats and PA-stimulated mouse primary hepatocytes. First, we tested liver and muscle glycogen contents in mice, and the data showed that liver and muscle glycogen levels were reduced in STZ/HFD mice (Fig. 2, A and B). OEA treatment increased liver and muscle glycogen contents in a dose-dependent manner, especially the up-regulation in hepatic glycogen levels (Fig. 2, A and B). PAS staining in the liver showed that OEA treatment (60 mg/kg)

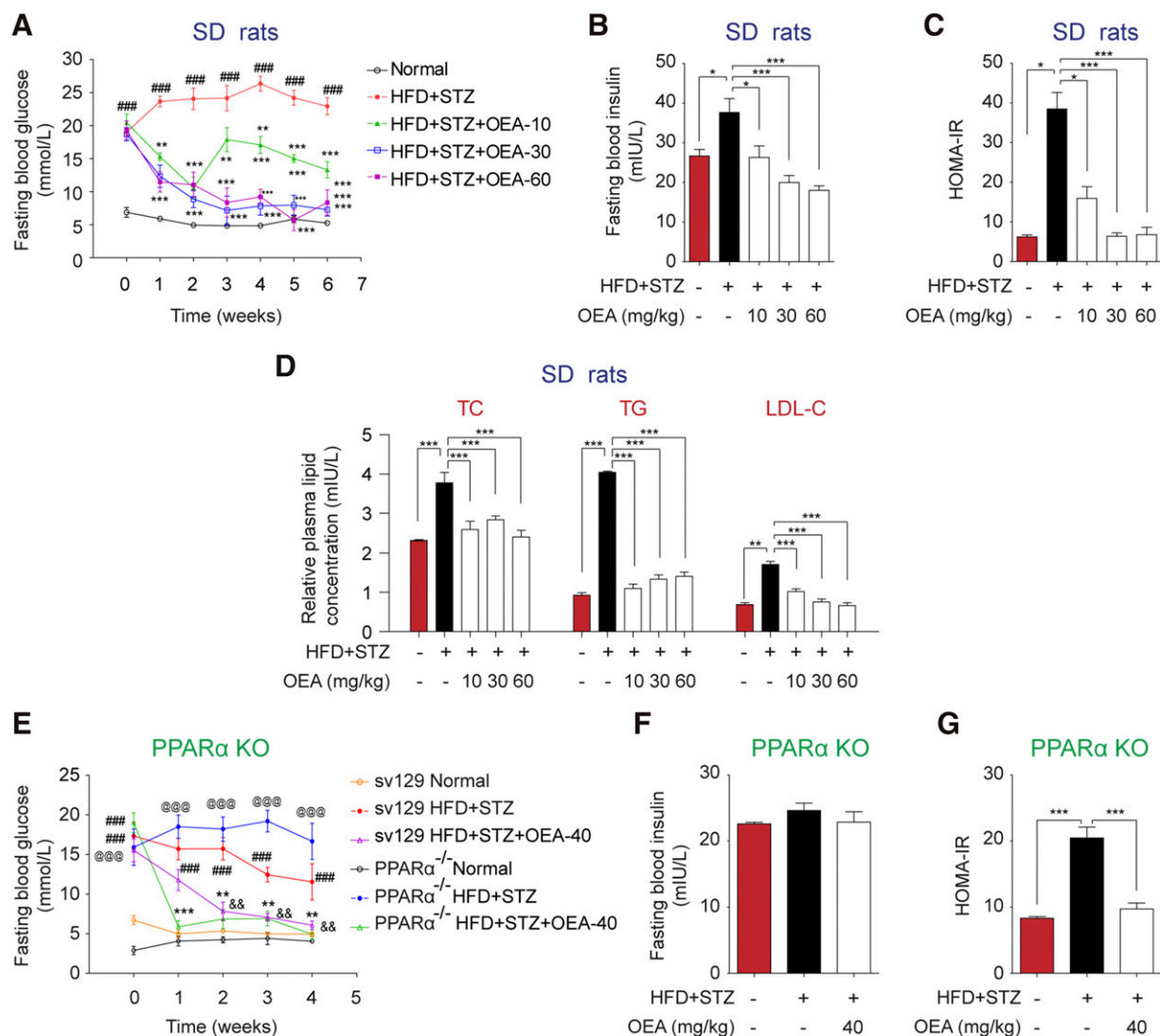


Fig. 1. OEA ameliorated hyperglycemia in a PPAR α -independent manner. OEA-treated groups received single daily intraperitoneal injections of OEA (10, 30, 60, or 40 mg/kg), and the normal and HFD/STZ groups were treated with vehicle on a daily basis. Glucose metabolites were measured using [(A) in diabetic rats; (E) in sv129 and PPAR α ^{-/-} mice] sequential monitoring of blood glucose after 8 hours of fasting, [(B) in diabetic rats; (F) in PPAR α ^{-/-} mice] fasting blood insulin, [(C) in diabetic rats; (G) in PPAR α ^{-/-} mice] levels of HOMA-IR, and (D) the levels of lipid homeostasis. Values are mean \pm S.E.M. ($n = 7$ or 6 per group). (A and E) [#] $P < 0.05$ vs. the normal (SD/sv129) group; ^{###} $P < 0.01$ vs. the normal (SD/sv129) group; ^{####} $P < 0.001$ vs. the normal (SD/sv129) group; ^{*} $P < 0.05$ vs. the HFD+STZ (SD/sv129) group; ^{**} $P < 0.01$ vs. the HFD+STZ (SD/sv129) group; ^{***} $P < 0.001$ vs. the HFD+STZ (SD/sv129) group; ^{@@@} $P < 0.001$ vs. the normal PPAR α ^{-/-} group; ^{&&} $P < 0.01$ vs. the HFD+STZ (SD/sv129) group. (B–D and F and G) ^{*} $P < 0.05$; ^{**} $P < 0.01$; ^{***} $P < 0.001$.

reversed STZ/HFD-induced hepatic glycogen down-regulation (Fig. 2C). OEA also promoted GSK3 β phosphorylation and inhibited PEPCK and G6Pase expression in mouse liver tissues (Fig. 2, D and E).

To elucidate the anti-IR effect of OEA on hepatocytes, PA was used to induce IR in mouse primary hepatocytes. PA-treated hepatocytes were induced with OEA (10, 20, and 40 μ M) for 24 hours, and glycogen concentration and glucose production were determined as metabolism markers. OEA treatment increased glycogen content and reduced glucose production (Fig. 3, A and B). OEA dose-dependently improved the PA-stimulated phosphorylation of GSK3 β (Fig. 3C) and down-regulated protein levels of G6Pase and PEPCK in primary hepatocytes (Fig. 3D). We found that 20 μ M OEA treatment resulted in the peak levels of metabolism markers in hepatocytes (Fig. 3, A and B). Therefore, the 20 μ M concentration of OEA was selected to

detect the optimal induction time of OEA in hepatocytes. OEA treatment enhanced glycogen at 12 hours, and this increase was sustained at 24 hours and reduced at 36 hours (Fig. 3E). OEA improved the PA-stimulated phosphorylation of GSK3 β in a time-dependent manner (Fig. 3G). OEA significantly reduced PA-stimulated glucose production and protein levels of G6Pase and PEPCK at 12 hours, which were sustained until 24 hours (Fig. 3, F and H). Taken together, OEA suppressed gluconeogenesis and accelerated glycogen synthesis in the liver.

OEA Regulated Liver Glucose Metabolism via LKB1/AMPK Signaling Pathways. Potential binding of the OEA digestive enzyme *N*-acyl ethanolamine acid amidase (NAAA) (Bandiera et al., 2014) and RNA-binding proteins to OEA were the predicted mechanisms of OEA regulation of liver glucose metabolism from the web (<http://priddb.gdcb.iastate.edu/RPISeq/>).

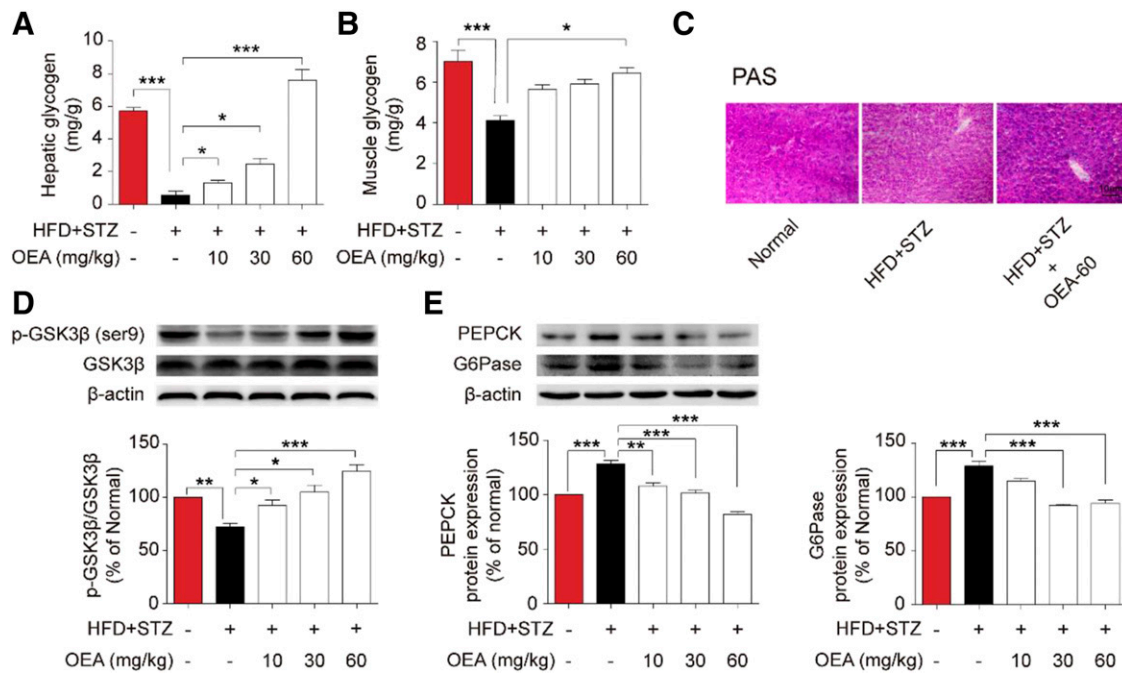


Fig. 2. Effects of OEA on hepatic gluconeogenesis and glycogenesis in diabetic rats. OEA-treated groups received single daily intraperitoneal injections of OEA (10, 30, or 60 mg/kg), and the normal and HFD/STZ groups were treated with vehicle on a daily basis. (A) Hepatic and (B) musculoskeletal glycogen contents. (C) Histologic analyses using PAS staining for hepatic glycogen in rat livers. Representative Western blot images of phosphorylated GSK3 β and GSK3 β and (D) quantitative analyses of phosphorylated GSK3 β to total GSK3 β in rat livers. (E) Representative Western blot images and quantitative analyses of protein expression of PEPCK and G6Pase in the livers of rats. The values are expressed as percentages compared with the normal group (set to 100%) and presented as the mean \pm S.E.M. ($n = 7$ per group), * $P < 0.05$; ** $P < 0.01$; *** $P < 0.001$.

NAAA exhibited a significant positive correlation with AMPK and LKB1 expression (Fig. 4, A and B). AMPK is a downstream gene of LKB1 that reduces hepatic glucose production and plasma glucose levels (Shackelford and Shaw, 2009). Therefore, the effect of OEA in regulating hepatic glucose metabolism is related to LKB1/AMPK pathways. The LKB1/AMPK pathways play a critical role in glucose metabolism and the pathogenesis of T2DM (Shaw et al., 2005). To determine the effect of AMPK and LKB1 on the antidiabetic effects of OEA, we tested the activities of AMPK and LKB1 in PA-stimulated primary hepatocytes and HFD/STZ-induced hepatic tissue of rats. We found that OEA up-regulated the phosphorylation of AMPK and LKB1 in both primary hepatocytes and hepatic tissue (Fig. 4, C and D), which suggests that OEA promotes the activation of AMPK and LKB1. Whether OEA is a direct activator of LKB1 needs further study.

Next, we further confirmed whether AMPK was involved in the effects of OEA in hepatic glycogen synthesis and gluconeogenesis. Primary hepatocytes were transiently transfected with AMPK siRNA for 24 hours, and the knock-down efficiency of AMPK was 66.02%, as determined by Western blot analysis (Fig. 5D). OEA increased glycogen synthesis in the negative controls in PA-stimulated hepatocytes, but AMPK siRNA obviously antagonized the increased effects of OEA on glycogen synthesis (Fig. 5A). OEA increased PA-induced p-GSK3 β levels in the negative control, but this effect was nearly abrogated in the AMPK siRNA cells (Fig. 5D). These results suggest that OEA increased hepatic glycogen synthesis in an AMPK-dependent manner. Furthermore, OEA decreased PA-induced glucose production and PEPCK and G6Pase levels in the negative control, but AMPK silencing

nearly reversed the suppressive effects of OEA on glucose production (Fig. 5B) and PEPCK and G6Pase expression (Fig. 5D). These results indicate a key role of AMPK in OEA regulation of gluconeogenesis. Therefore, our results suggest that OEA regulates hepatic glycogen synthesis and gluconeogenesis via an AMPK pathway.

Considering the regulation of LKB1/AMPK on gluconeogenesis (Miller et al., 2011; Patel et al., 2014; Duca et al., 2015) and the effect of OEA on activation of AMPK signal, we further examined the role of LKB1 in OEA regulation of glycogen synthesis and gluconeogenesis. As shown in Fig. 5, E and F, the LKB1 inhibitor Pim1/AKK-IN-1 (Bamborough et al., 2008) reversed the effects of OEA on glycogen content and glucose production. OEA enhanced the phosphorylation of LKB1, AMPK, and GSK3 β and inhibited PEPCK and G6Pase expression in PA-stimulated primary hepatocytes, but Pim1/AKK-IN-1 treatment nearly abrogated these effects (Fig. 5, G and H), which suggests that OEA regulated hepatic glycogen synthesis and gluconeogenesis via LKB1/AMPK pathways.

OEA Activated LKB1/AMPK Pathways in a PPAR α -Independent Manner. We further examined whether PPAR α was associated with AMPK/LKB1 signaling. We detected the activities of AMPK and LKB1 in PPAR α KO mice. The data revealed that OEA treatment up-regulated the phosphorylation of LKB1 and AMPK in liver tissues of HFD/STZ PPAR α KO mice (Fig. 6, A–C), which indicates that OEA activated AMPK and LKB1 signals in PPAR α KO mice. Therefore, the OEA-induced activation of LKB1 and AMPK is not related to PPAR α signal.

OEA promotes hepatic glycogen synthesis and inhibits gluconeogenesis, but PPAR α is not involved in the regulation of OEA on glucose metabolism. Therefore, KEGG pathway

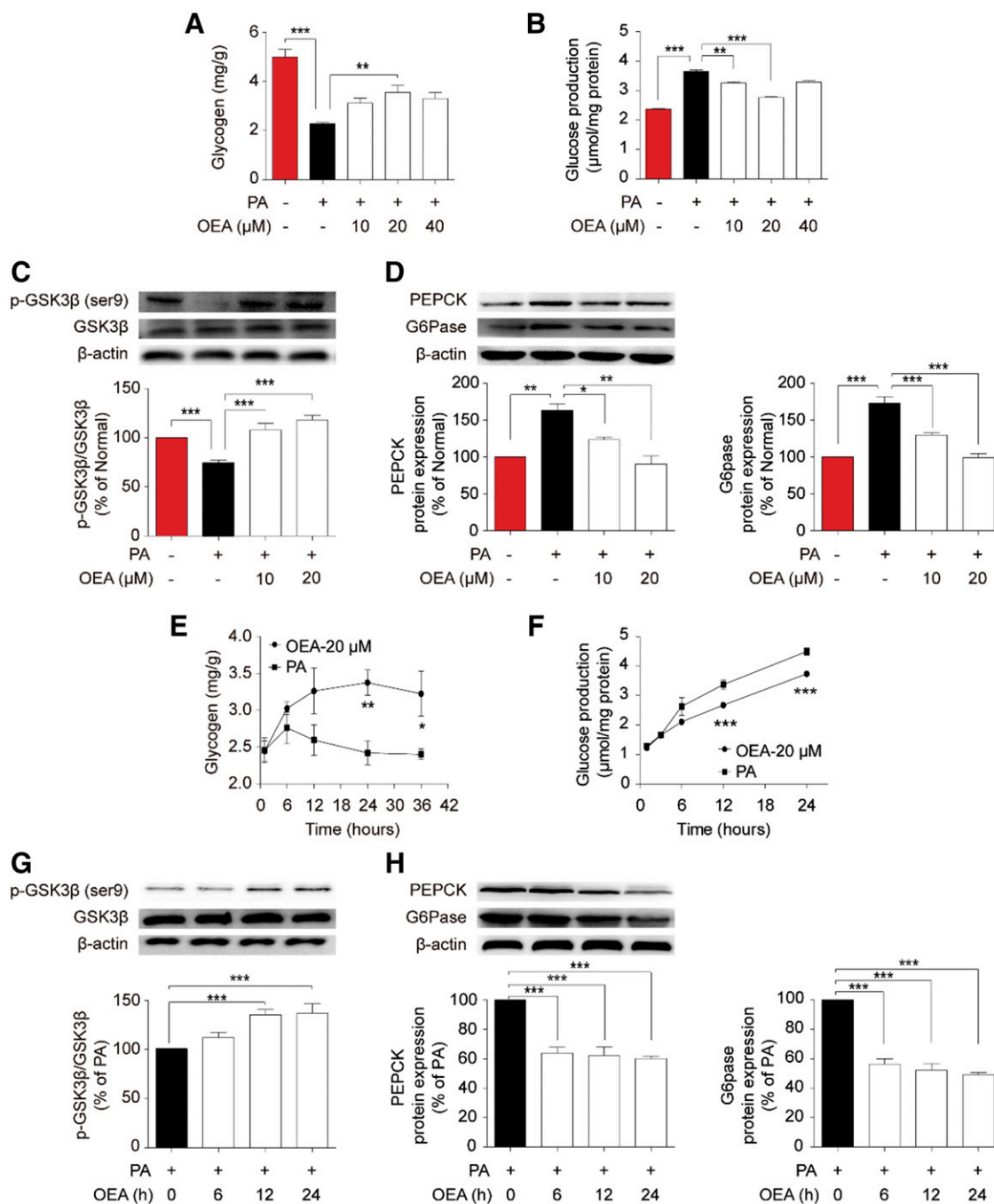


Fig. 3. Effects of OEA on hepatic gluconeogenesis and glycogenesis in PA-stimulated mouse primary hepatocytes. OEA-treated cells received different concentrations of OEA (10, 20, or 40 μ M) for 24 hours or 20 μ M OEA for different times (3, 6, 12, 24, or 36 hours), and the normal and PA-stimulated cells were treated with vehicle. Glucose metabolites were measured for (A and E) glycogen content and (B and F) glucose production. (C, D, G, and H) Representative Western blot images of phosphorylated GSK3 β , GSK3 β , PEPCK, and G6Pase and quantitative analyses of phosphorylated GSK3 β to total GSK3 β and the protein expression of PEPCK and G6Pase. The values are expressed as percentages compared with the normal group (set to 100%) and presented as the mean \pm S.E.M. ($n = 4$ per group), * $P < 0.05$; ** $P < 0.01$; *** $P < 0.001$.

enrichment was performed via analysis of PPAR α in the GSE13760 dataset. Correlations between PPAR α levels and GSK3 β , PEPCK, G6Pase, and LKB1 or AMPK in patients with GSE13760 T2DM were examined. PPAR α did not correlate with GSK3 β or PEPCK gene expression (Fig. 6, D and E). However, PPAR α exhibited a significant positive correlation with G6Pase gene expression (Fig. 6F). These results suggest that OEA improved hepatic IR in a PPAR α -independent manner. PPAR α was not significantly correlated with AMPK

or LKB1 (Fig. 6, G and H), which further suggests that OEA activation of AMPK and LKB1 is not related to PPAR α . Taken together, these data suggest that PPAR α is not involved in OEA regulation of glucose metabolism.

GPR119 plays a key role in glucose and lipid metabolism, and OEA is one of the most active ligands of GPR119. Therefore, we further explore whether GPR119 is involved in the roles of OEA in hepatic glycogen synthesis and gluconeogenesis. We found that OEA treatment significantly up-regulated the mRNA

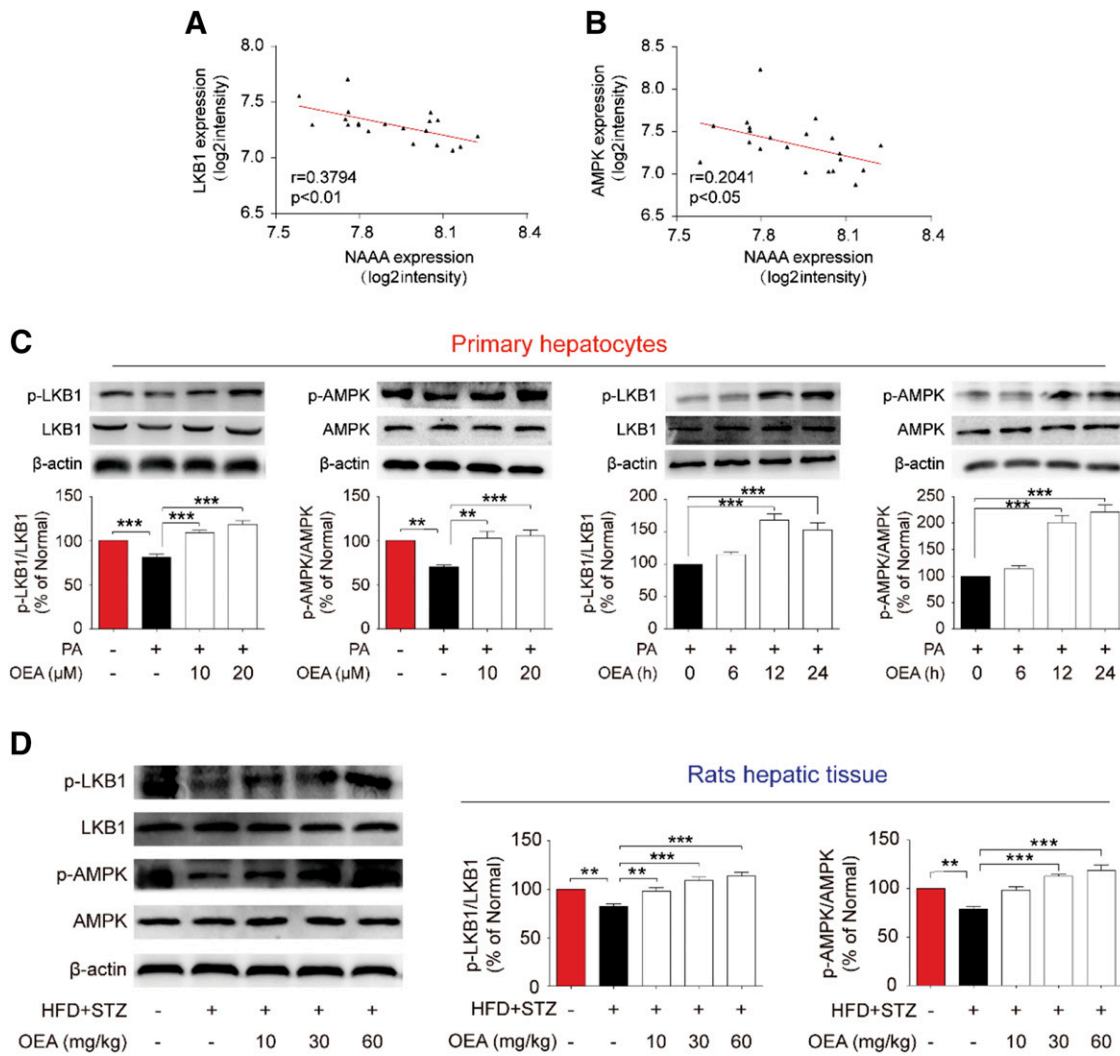


Fig. 4. OEA promoted the activation of AMPK and LKB1 signals. (A and B) The relationship between NAAA expression and LKB1 or AMPK mRNA levels was analyzed in profiles of samples from patients with T2DM from GSE13760. (C) OEA-treated cells received different concentrations of OEA (10, 20, or 40 μ M) for 24 hours or 20 μ M OEA for different times (3, 6, 12, 24, or 36 hours), and the normal and PA-stimulated cells were treated with vehicle. (D) OEA-treated groups received single daily intraperitoneal injections of OEA (10, 30, or 60 mg/kg), and the normal and HFD/STZ rats were treated with vehicle on a daily basis. Representative Western blot images and quantitative analyses of phosphorylated LKB1 to total LKB1 and phosphorylated AMPK to total AMPK. The values are expressed as percentages compared with the normal group (set to 100%) and presented as the mean \pm S.E.M. ($n = 4$ per group), * $P < 0.05$; ** $P < 0.01$; *** $P < 0.001$.

expression of GPR119 and glucagon-like peptide-1 level in PA-induced primary hepatocytes (Supplemental Fig. 4, A–D). Additionally, GPR119 siRNA obviously antagonized the effect of OEA on glucose production but not on glycogen synthesis (Supplemental Fig. 4, F and G). Furthermore, we compare the effects of OEA and another GPR119 agonist, PSN632408, on glycogen synthesis and glucose production. The results show that OEA up-regulated glycogen levels, but PSN632408 had no effect on glycogen synthesis (Supplemental Fig. 4H). However, both OEA and PSN632408 markedly decreased glucose production in PA-stimulated hepatocytes (Supplemental Fig. 4I). Meanwhile, we further examined the role of CB1 in OEA regulation of glycogen synthesis and gluconeogenesis. As shown in Supplemental Fig. 5, A and B, CB1 mRNA were significantly up-regulated by OEA in PA-induced primary hepatocytes. CB1 inhibitor otenabant reversed the effect of OEA on glucose production but not on glycogen content (Supplemental Fig. 5, C–E).

These data suggest that OEA reduced glycogen synthesis independent of GPR119 and CB1 pathways.

Discussion

The salient findings of this study are that: 1) OEA improved glucose homeostasis in a PPAR α -independent manner, 2) OEA exerted an antihyperglycemic effect primarily via regulation of hepatic glycogen synthesis and gluconeogenesis, and 3) the main molecular mechanism of OEA in regulating liver glucose metabolism is to regulate LKB1/AMPK signaling pathway.

Several reports indicated that a PPAR α agonist suppressed obesity-induced glucose metabolism abnormalities in animal models (Kang et al., 2010; Park et al., 2016; Jeong et al., 2018). Previous clinical studies showed that PPAR α agonists, fibrates, may be useful for the treatment of disorders of glucose metabolism in noninsulin-dependent diabetes (Malur et al., 2017;

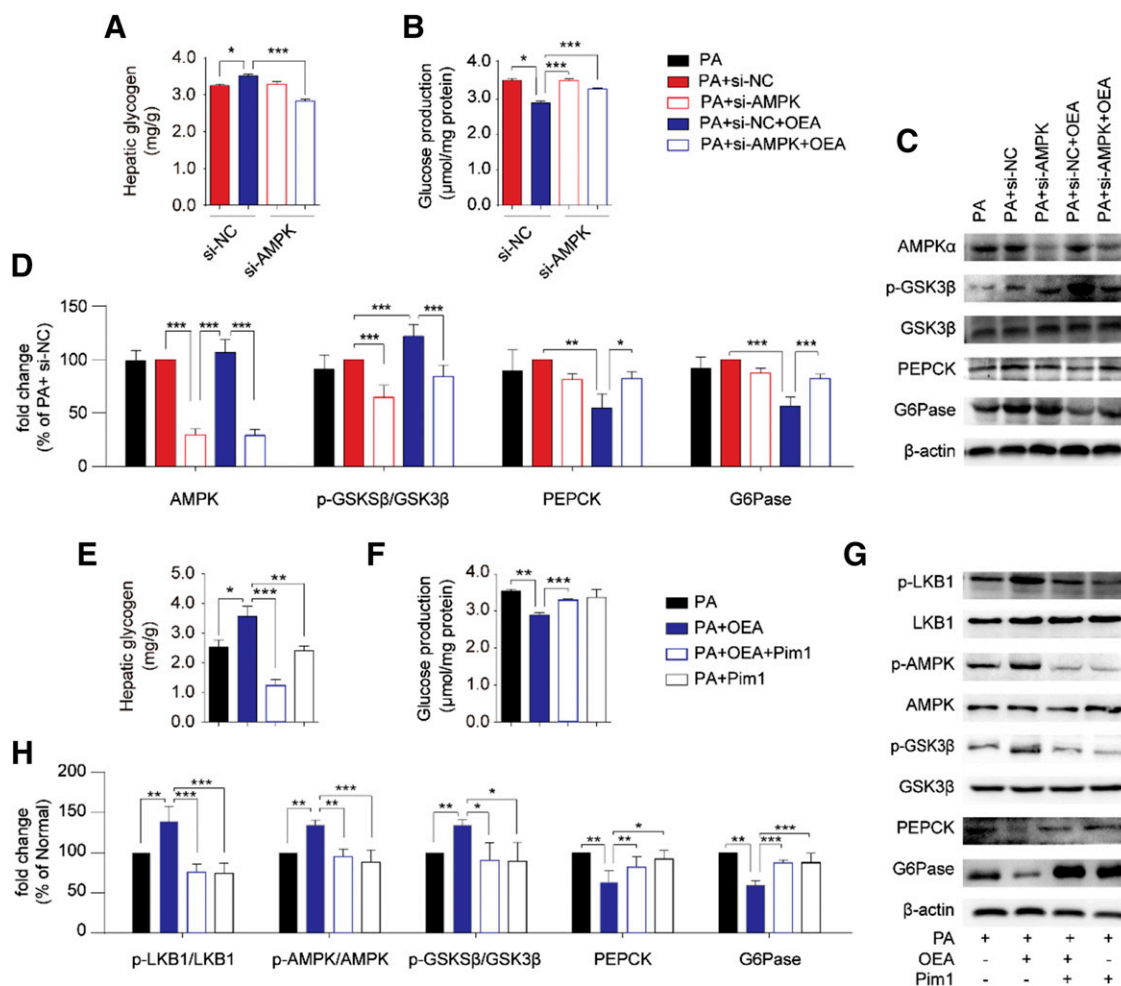


Fig. 5. OEA regulated liver glucose metabolism via LKB1/AMPK signaling pathways. (A–D) Primary hepatocytes were transfected with siRNA–negative control or siRNA-AMPK for 72 hours, which was followed by OEA (20 μM) treatment of an additional 12 hours. (E–H) Primary hepatocytes were treated with the LKB1 inhibitor Pim1/AKK1-IN-1 (Pim1) (380 nM) for 12 hours, followed by OEA (20 μM) treatment of an additional 12 hours. The values are expressed as percentages compared with normal group (set to 100%) and presented as the mean ± S.E.M. of five separate experiments performed in duplicate ($n = 4$ per group), * $P < 0.05$; ** $P < 0.01$; *** $P < 0.001$. NC, negative control.

Yuan et al., 2019). OEA is an endogenous ligand of PPAR α , and it plays vital roles in reducing food intake and promoting lipid catabolism. In the present study, we found that OEA did not reduce serum hyperlipidemia in HFD/STZ-induced PPAR α KO mice, which indicates that PPAR α also plays a crucial role in regulating lipid metabolism in DM. OEA regulates glucose uptake in isolated adipocytes (Guzmán et al., 2004). Our latest research demonstrate that OEA suppressed plasma glucose and reduced hippocampal disturbances of glucose metabolism in diabetic mice (Ren et al., 2019). However, the role of PPAR α in OEA regulation of glucose metabolism is not clear. The present study used the HFD/STZ-induced diabetic model in PPAR α KO mice and found that PPAR α KO mice also developed DM after 6 weeks of HFD and a single dose of STZ management, which is consistent with a previous report (Neschen et al., 2007). This result indicates that PPAR α is not a necessary factor in the pathologic development of DM. Notably, we found that OEA efficiently suppressed hyperglycemia and hyperinsulinemia in HFD/STZ-induced diabetic PPAR α KO mice, which supports a PPAR α -independent mechanism of OEA blood sugar regulation in diabetes. Therefore, our data suggest that OEA

reduces blood glucose levels in DM via a PPAR α -independent mechanism. However, previous studies showed that OEA impaired glucose tolerance and inhibited insulin-stimulated glucose uptake in rat adipocytes (González-Yanes et al., 2005). Several reasons may explain the differences between these results and our data. First, the other studies tested the effect of OEA on blood sugar in healthy rats, whereas we focused on HFD/STZ-induced diabetic animals. Second, the other studies were primarily concerned with sugar uptake in adipose tissue, whereas we examined blood sugar levels in vivo. Third, the other studies gave an acute administration of OEA (30 minutes and 6 hours), whereas we used chronic administration (6 weeks). Previous studies reported that the PPAR α agonists fenofibrate and gemfibrozil produced impairment of glucose tolerance and a moderate increase of fasting blood glucose in rats (Ohrvall et al., 1995; Liu et al., 2011). We found that, unlike with fenofibrate, there were no changes in glucose tolerance between the OEA-treated and vehicle-treated mice (see Supplemental Fig. 6), which suggests that long-term OEA administration did not impair glucose tolerance. Taken together, our data indicate that the antihyperglycemic effects of OEA in DM are PPAR α independent.

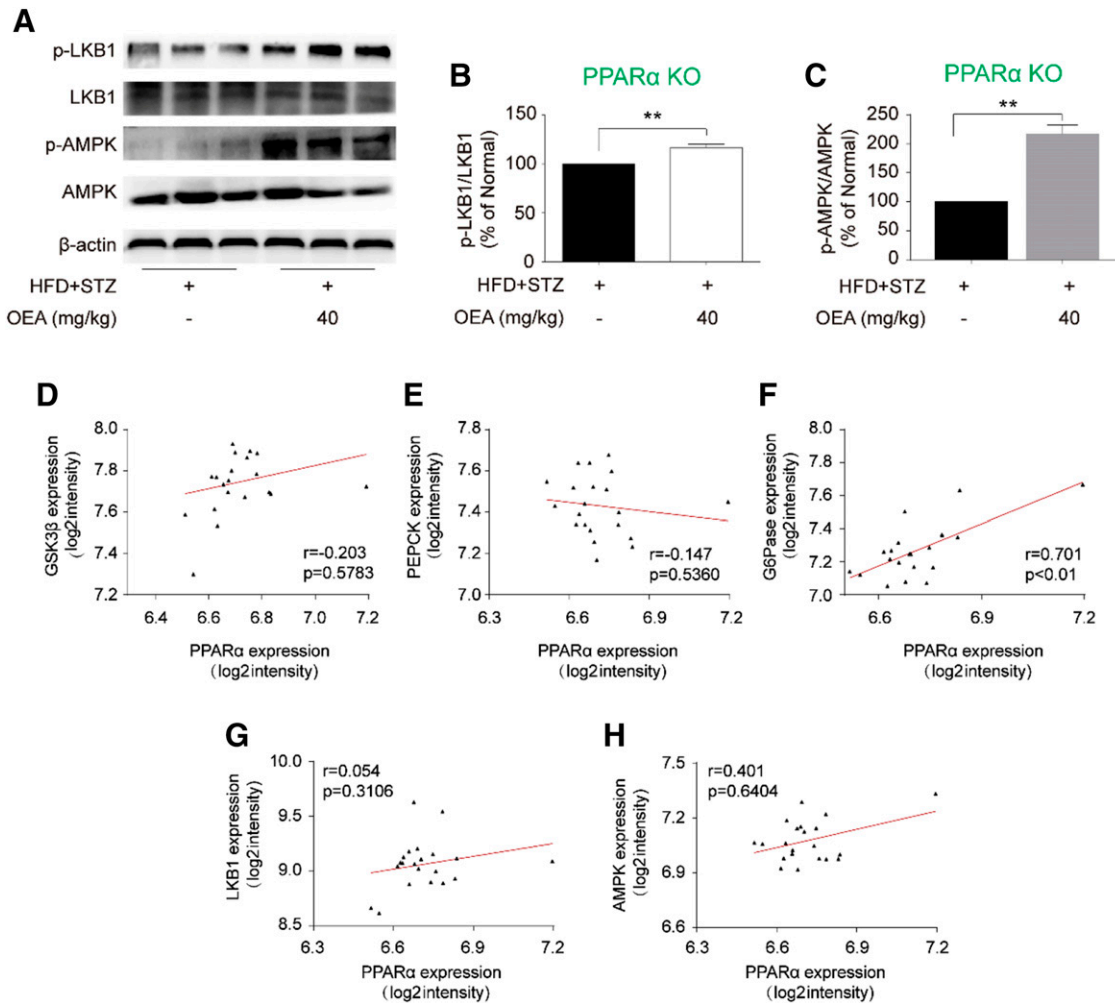


Fig. 6. OEA activated LKB1/AMPK pathways in a PPAR α -independent manner. (A–C) OEA-treated groups received single daily intraperitoneal injections of OEA (40 mg/kg), and the HFD/STZ groups were treated with vehicle on a daily basis. Representative Western blot images and quantitative analyses of phosphorylated LKB1 to total LKB1 and phosphorylated AMPK to total AMPK. Values are mean \pm S.E.M. ($n = 3$ per group), ** $P < 0.01$. (D–H) The relationship between PPAR α expression and GSK3 β , PEPCK, G6Pase, LKB1, and AMPK mRNA levels was analyzed in profiles of samples from patients with T2DM from GSE13760. The mean values and S.D. were calculated from triplicates of a representative experiment.

In addition to adipose tissue and skeletal muscle, the liver is also a main target organ for the regulation of glucose metabolism. The liver is primarily responsible for maintaining blood glucose levels via gluconeogenesis and glycogen synthesis (Santiago-Martínez et al., 2016). Hepatic insulin resistance in patients with diabetes results in a decline of hepatic glycogen storage and glycogen synthase activity (Nordlie et al., 1999; Barthel and Schmolz, 2003). Abundant hepatic glucose production is a major determinant of fasting hyperglycemia in type 2 diabetes. Hepatic insulin resistance in diabetes directly leads to reduce the ability of insulin to inhibit hepatic gluconeogenesis and enhance hepatic glucose production (Petersen et al., 2017). Therefore, the increase of glycogen storage via the promotion of glycogen synthase activity or the reduction in glucose production via gluconeogenesis suppression is a therapeutic target in T2DM (Ismail, 2018). Results of the present study showed that OEA treatment increased glycogen synthesis and storage and inhibited gluconeogenesis and endogenous glucose production in primary hepatocytes and liver tissue. These results suggest that OEA reduces fasting blood glucose and insulin resistance

through regulating hepatic gluconeogenesis and glycogen synthesis in type 2 diabetes. Additionally, we also compared the effects of OEA and metformin on glucose production and glycogen synthesis. PA-stimulated primary hepatocytes were treated with 20 μ M of OEA and metformin, and we found that there was no difference in increasing glycogen and glucose production between OEA and metformin (Supplemental Fig. 7, A and B). However, we only compared one dose of two drugs in the present study, and the comparison of them on regulation of glucose metabolism need to be further study.

GSK3 plays a critical role in insulin resistance via the inhibition of glycogen synthase activity (Dong et al., 2016). Ser-phosphorylation at S21 and S9 inactivates GSK-3 α and β , respectively, which enhances insulin-stimulated glycogen synthesis (Cohen and Frame, 2001). GSK3 antagonists improve glucose metabolism via increasing hepatic glycogen levels, which suggests that the inhibition of GSK3 is a potential therapy for the treatment of insulin resistance and type 2 diabetes. Here, we found that OEA increased hepatic glycogen synthesis via inhibition of GSK activity. This pathway is similar to the role of insulin in promoting glycogen synthesis.

Glucose isogenic targets PEPCK and G6Pase are closely related to hepatic glucose production. Oral hypoglycemic drugs, such as biguanides, thiazolidinediones, and sulfonylureas, primarily reduce glucose production via inhibition of PEPCK and G6Pase (He et al., 2016). Our data indicate that OEA inhibited PEPCK and G6Pase expression, which is similar to how the signaling pathway of metformin plays into the suppression of gluconeogenesis.

AMPK is a central metabolic switch found in all eukaryotes that governs glucose and lipid metabolism in response to alterations in nutrients and intracellular energy levels (Woods et al., 2017). AMPK controls two critical liver functions, gluconeogenesis and lipogenesis, and it is activated when ATP decreases and AMP concentrations increase in response to nutrient deprivation and pathologic stresses. A previous report revealed the role of AMPK in improving hepatic glycogen metabolism (Viollet, 2017). For example, metformin activates AMPK and reduces hepatic glucose production, exenatide exerts direct protective effects on glucose intolerance, and rosiglitazone enhances glycolysis and glucose uptake (Foretz et al., 2010). When levels of ATP, glucose, or oxygen are low, AMPK primes nearby serine residues for subsequent phosphorylation by GSK-3 (Suzuki et al., 2013). Several studies demonstrated that AMPK activation induces insulin sensitization and promotes glucose intake via GSK-3 β regulation (Kong et al., 2019). Notably, AMPK reduces hepatic glucose production via decreasing PEPCK and G6Pase expression. In the present study, we found that OEA inhibited gluconeogenesis and enhanced glycogen synthase in hepatocytes via an AMPK-dependent pathway, which is consistent with metformin reduction of hepatic glycogen synthesis via enhancing AMPK phosphorylation in diabetic rat liver. Therefore, AMPK is one of the main targets of OEA in the regulation of hepatic glycogen metabolism.

Another important finding of our study is that OEA regulated the LKB1 signal in hepatocytes and liver tissue with insulin resistance. LKB1 is a master upstream kinase that directly phosphorylates and activates AMPK and a family of 12 related kinases that play critical roles in cell growth, metabolism, and polarity (Shaw et al., 2005). LKB1 is inactivated under a chronic hyperglycemic state. Therefore, LKB1 activation may be a significant strategy to stimulate glucose uptake and fatty acid oxidation. Loss of LKB1 function resulted in hyperglycemia with increased gluconeogenic and lipogenic gene expression. Previous studies showed that blood sugar and insulin levels in liver LKB1-deficient mice increased over time (Bang et al., 2014), which suggests that LKB1 plays an important role in the regulation of blood sugar and insulin homeostasis. LKB1 in liver is required for the ability of metformin to lower blood glucose. The LKB1 kinase is genetically required for AMPK activation by energy stress in different kinds of mammalian cell lines. Chronic metformin activates liver AMPK and reduces plasma glucose levels in diabetic rodents (Park et al., 2002). In the present study, the data shows that the LKB1 inhibitor Pim1/AKK-IN-1 reversed the efficiency of OEA in hepatic glycogen synthesis and glucose production, suggesting that OEA inhibited gluconeogenesis and increased glycogen synthase in hepatocytes via an LKB1-dependent pathway. Additionally, Pim1/AKK-IN-1 blocked OEA-induced AMPK activity, which indicates that OEA regulates AMPK activity through the LKB1 pathway. Therefore, OEA enhances hepatic glycogen synthesis and

inhibits gluconeogenesis in an LKB1/AMPK-dependent manner, which suggests that LKB1/AMPK signaling is an important mechanism of OEA regulation of glucose metabolism.

To further elucidate the role of PPAR α in OEA glucose metabolism, KEGG pathway enrichment analysis was performed via analyses of PPAR α in the GSE13760 dataset. The results revealed that PPAR α was not correlated with GSK3 β or PEPCK gene expression, which suggests that OEA regulation of glycogen synthesis and gluconeogenesis are independent of the PPAR α pathway. Moreover, the results from PPAR α KO mice and enrichment analysis indicated the effect of OEA on regulation of LKB1 and AMPK signaling independent of PPAR α pathway. These results further indicated that the regulatory effects of OEA on glucose metabolism in diabetes mellitus are not related to PPAR α signal.

Conclusions

Our findings indicate that OEA attenuated hyperglycemia and insulin resistance in a PPAR α -independent manner. The hypoglycemic effect of OEA primarily occurred via the regulation of hepatic glycogen synthesis and gluconeogenesis via activation of LKB1/AMPK signaling. These findings provide new insight into the pharmacologic usefulness of OEA.

Acknowledgments

The authors thank Xie Baoying (Central Laboratory, Xiamen University) for her help in providing pharmacokinetic analysis.

Authorship Contributions

Participated in research design: Yao, Yang.
Conducted experiments: Ren, Ma, Zhuo, Zhang, Peng.
Contributed new reagents or analytic tools: Ren, Ma, Zhuo, Zhang, Peng.
Performed data analysis: Jin.
Wrote or contributed to the writing of the manuscript: Yang, Ren.

References

- Annuzzi G, Piscitelli F, Di Marino L, Patti L, Giacco R, Costabile G, Bozzetto L, Riccardi G, Verde R, Petrosino S, et al. (2010) Differential alterations of the concentrations of endocannabinoids and related lipids in the subcutaneous adipose tissue of obese diabetic patients. *Lipids Health Dis* 9:43.
- Assmann TS, Recamonde-Mendoza M, De Souza BM, and Crispim D (2017) Micro-RNA expression profiles and type 1 diabetes mellitus: systematic review and bioinformatic analysis. *Endocr Connect* 6:773–790.
- Bamborough P, Drewry D, Harper G, Smith GK, and Schneider K (2008) Assessment of chemical coverage of kinome space and its implications for kinase drug discovery. *J Med Chem* 51:7898–7914.
- Bandiera T, Ponzano S, and Piomelli D (2014) Advances in the discovery of N-acylethanolamine acid amidase inhibitors. *Pharmacol Res* 86:11–17.
- Bang S, Chen Y, Ahima RS, and Kim SF (2014) Convergence of IPMK and LKB1-AMPK signaling pathways on metformin action. *Mol Endocrinol* 28:1186–1193.
- Barthel A and Schmol D (2003) Novel concepts in insulin regulation of hepatic gluconeogenesis. *Am J Physiol Endocrinol Metab* 285:E685–E692.
- Brown JD, Karimian Azari E, and Ayala JE (2017) Oleylethanolamide: a fat ally in the fight against obesity. *Physiol Behav* 176:50–58.
- Cohen P and Frame S (2001) The renaissance of GSK3. *Nat Rev Mol Cell Biol* 2:769–776.
- Danaei G, Finucane MM, Lu Y, Singh GM, Cowan MJ, Paciorek CJ, Lin JK, Farzadfar F, Khang YH, Stevens GA, et al.; Global Burden of Metabolic Risk Factors of Chronic Diseases Collaborating Group (Blood Glucose) (2011) National, regional, and global trends in fasting plasma glucose and diabetes prevalence since 1980: systematic analysis of health examination surveys and epidemiological studies with 370 country-years and 2.7 million participants. *Lancet* 378:31–40.
- Dong Z, Luo Y, Cai H, Zhang Z, Peng Z, Jiang M, Li Y, Li C, Li ZP, and Feng ST (2016) Noninvasive fat quantification of the liver and pancreas may provide potential biomarkers of impaired glucose tolerance and type 2 diabetes. *Medicine (Baltimore)* 95:e3858.
- Duca FA, Côté CD, Rasmussen BA, Zadeh-Tahmasebi M, Rutter GA, Filippi BM, and Lam TK (2015) Metformin activates a duodenal Ampk-dependent pathway to lower hepatic glucose production in rats. *Nat Med* 21:506–511.
- Foretz M, Hébrard S, Leclerc J, Zarrinpashneh E, Soty M, Mithieux G, Sakamoto K, Andreelli F, and Viollet B (2010) Metformin inhibits hepatic gluconeogenesis in mice independently of the LKB1/AMPK pathway via a decrease in hepatic energy state. *J Clin Invest* 120:2355–2369.

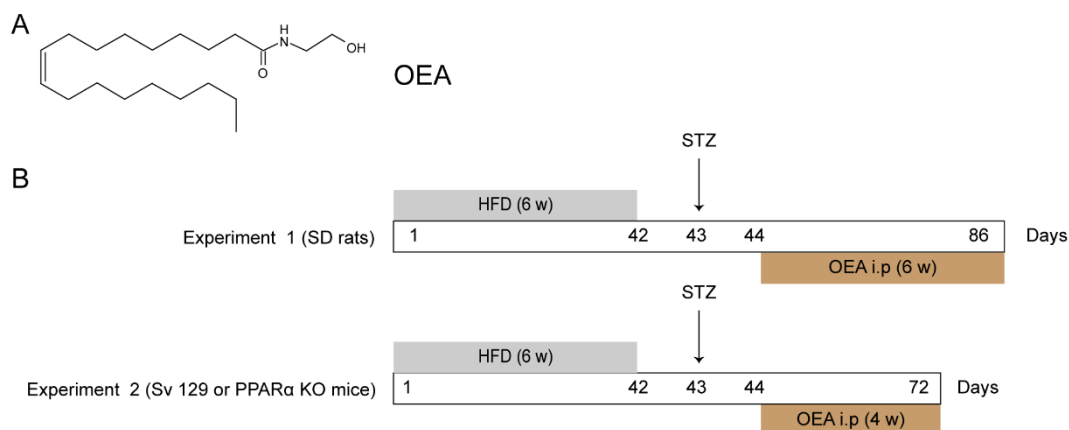
- Fu J, Gaetani S, Oveisi F, Lo Verme J, Serrano A, Rodríguez De Fonseca F, Rosegarth A, Luecke H, Di Giacomo B, Tarzia G, et al. (2003) Oleylethanolamide regulates feeding and body weight through activation of the nuclear receptor PPAR- α . *Nature* **425**:90–93.
- Gaetani S, Kaye WH, Cuomo V, and Piomelli D (2008) Role of endocannabinoids and their analogues in obesity and eating disorders [published correction appears in *Eat Weight Disord* (2011) 16:e72]. *Eat Weight Disord* **13**:e42–e48.
- Gilbert ER, Fu Z, and Liu D (2011) Development of a nongenetic mouse model of type 2 diabetes. *Exp Diabetes Res* **2011**:416254.
- González-Yanes C, Serrano A, Bermúdez-Silva FJ, Hernández-Domínguez M, Páez-Ochoa MA, Rodríguez de Fonseca F, and Sánchez-Margalet V (2005) Oleylethanolamide impairs glucose tolerance and inhibits insulin-stimulated glucose uptake in rat adipocytes through p38 and JNK MAPK pathways. *Am J Physiol Endocrinol Metab* **289**:E923–E929.
- Grundy SM (2015) Adipose tissue and metabolic syndrome: too much, too little or neither. *Eur J Clin Invest* **45**:1209–1217.
- Guzmán M, Lo Verme J, Fu J, Oveisi F, Blázquez C, and Piomelli D (2004) Oleylethanolamide stimulates lipolysis by activating the nuclear receptor peroxisome proliferator-activated receptor α (PPAR- α). *J Biol Chem* **279**:27849–27854.
- Hausler RA, Hartil K, Vaitheesvaran B, Arrieta-Cruz I, Knight CM, Cook JR, Kammoun HL, Febbraio MA, Gutierrez-Juarez R, Kurland LJ, et al. (2014) Integrated control of hepatic lipogenesis versus glucose production requires FoxO transcription factors. *Nat Commun* **5**:5190.
- He L, Chang E, Peng J, An H, McMillin SM, Radovick S, Stratakis CA, and Wondisford FE (2016) Activation of the cAMP-PKA pathway antagonizes metformin suppression of hepatic glucose production. *J Biol Chem* **291**:10562–10570.
- Ismail IS (2018) The role of carbonic anhydrase in hepatic glucose production. *Curr Diabetes Rev* **14**:108–112.
- Jeong JW, Lee B, Kim DH, Jeong HO, Moon KM, Kim MJ, Yokozawa T, and Chung HY (2018) Mechanism of action of magnesium lithospermate B against aging and obesity-induced ER stress, insulin resistance, and inflammable formation in the liver. *Molecules* **23**:E2098.
- Kang JH, Goto T, Han IS, Kawada T, Kim YM, and Yu R (2010) Dietary capsaicin reduces obesity-induced insulin resistance and hepatic steatosis in obese mice fed a high-fat diet. *Obesity (Silver Spring)* **18**:780–787.
- Kong D, Hua X, Qin T, Zhang J, He K, and Xia Q (2019) Inhibition of glycogen synthase kinase 3 β protects liver against ischemia/reperfusion injury by activating 5' adenosine monophosphate-activated protein kinase-mediated autophagy. *Hepatology Res* **49**:462–472.
- Liu SN, Liu Q, Li LY, Huan Y, Sun SJ, and Shen ZF (2011) Long-term fenofibrate treatment impaired glucose-stimulated insulin secretion and up-regulated pancreatic NF- κ B and iNOS expression in monosodium glutamate-induced obese rats: is that a latent disadvantage? *J Transl Med* **9**:176.
- Liu TY, Shi CX, Gao R, Sun HJ, Xiong XQ, Ding L, Chen Q, Li YH, Wang JJ, Kang YM, et al. (2015) Irisin inhibits hepatic gluconeogenesis and increases glycogen synthesis via the PI3K/Akt pathway in type 2 diabetic mice and hepatocytes. *Clin Sci (Lond)* **129**:839–850.
- Malur P, Menezes A, DiNicolantonio JJ, O'Keefe JH, and Lavie CJ (2017) The microvascular and macrovascular benefits of fibrates in diabetes and the metabolic syndrome: a review. *Mo Med* **114**:464–471.
- Martínez de Ubago M, García-Oya I, Pérez-Pérez A, Canfrán-Duque A, Quintana-Portillo R, Rodríguez de Fonseca F, González-Yanes C, and Sánchez-Margalet V (2009) Oleylethanolamide, a natural ligand for PPAR- α , inhibits insulin receptor signalling in HTC rat hepatoma cells. *Biochim Biophys Acta* **1791**:740–745.
- McKillop AM, Moran BM, Abdel-Wahab YH, and Flatt PR (2013) Evaluation of the insulin releasing and antihyperglycaemic activities of GPR55 lipid agonists using clonal beta-cells, isolated pancreatic islets and mice. *Br J Pharmacol* **170**:978–990.
- Miller RA, Chu Q, Le Lay J, Scherer PE, Ahima RS, Kaestner KH, Foretz M, Viollet B, and Birnbaum MJ (2011) Adiponectin suppresses gluconeogenic gene expression in mouse hepatocytes independent of LKB1-AMPK signaling. *J Clin Invest* **121**:2518–2528.
- Miller RA, Chu Q, Xie J, Foretz M, Viollet B, and Birnbaum MJ (2013) Biguanides suppress hepatic glucagon signalling by decreasing production of cyclic AMP. *Nature* **494**:256–260.
- Moore MC, Smith MS, Farmer B, Coate KC, Kraft G, Shiota M, Williams PE, and Cherrington AD (2018) Morning hyperinsulinemia primes the liver for glucose uptake and glycogen storage later in the day. *Diabetes* **67**:1237–1245.
- Neschen S, Morino K, Dong J, Wang-Fischer Y, Cline GW, Romanelli AJ, Rossbacher JC, Moore IK, Regittinig W, Munoz DS, et al. (2007) n-3 Fatty acids preserve insulin sensitivity in vivo in a peroxisome proliferator-activated receptor- α -dependent manner. *Diabetes* **56**:1034–1041.
- Nordlie RC, Foster JD, and Lange AJ (1999) Regulation of glucose production by the liver. *Annu Rev Nutr* **19**:379–406.
- Ohrvall M, Lithell H, Johansson J, and Vessby B (1995) A comparison between the effects of gemfibrozil and simvastatin on insulin sensitivity in patients with non-insulin-dependent diabetes mellitus and hyperlipoproteinemia. *Metabolism* **44**:212–217.
- Park H, Kaushik VK, Constant S, Prentki M, Przybytkowski E, Ruderman NB, and Saha AK (2002) Coordinate regulation of malonyl-CoA decarboxylase, sn-glycerol-3-phosphate acyltransferase, and acetyl-CoA carboxylase by AMP-activated protein kinase in rat tissues in response to exercise. *J Biol Chem* **277**:32571–32577.
- Park HS, Hur HJ, Kim SH, Park SJ, Hong MJ, Sung MJ, Kwon DY, and Kim MS (2016) Biochanin A improves hepatic steatosis and insulin resistance by regulating the hepatic lipid and glucose metabolic pathways in diet-induced obese mice. *Mol Nutr Food Res* **60**:1944–1955.
- Pastor A, Farré M, Fitó M, Fernandez-Aranda F, and de la Torre R (2014) Analysis of ECs and related compounds in plasma: artifactual isomerization and ex vivo enzymatic generation of 2-MGs. *J Lipid Res* **55**:966–977.
- Patel K, Foretz M, Marion A, Campbell DG, Gourlay R, Boudaba N, Tournier E, Titchenell P, Peggie M, Deak M, et al. (2014) The LKB1-salt-inducible kinase pathway functions as a key gluconeogenic suppressor in the liver. *Nat Commun* **5**:4535.
- Petersen MC, Vatner DF, and Shulman GI (2017) Regulation of hepatic glucose metabolism in health and disease. *Nat Rev Endocrinol* **13**:572–587.
- Ren T, Liu J, Ge Y, Zhuo R, Peng L, Liu F, Jin X, and Yang L (2019) Chronic oleylethanolamide treatment attenuates diabetes-induced mice encephalopathy by triggering peroxisome proliferator-activated receptor α in the hippocampus. *Neurochem Int* **129**:104501.
- Santiago-Martínez MG, Encalada R, Lira-Silva E, Pineda E, Gallardo-Pérez JC, Reyes-García MA, Saavedra E, Moreno-Sánchez R, Marín-Hernández A, and Jasso-Chávez R (2016) The nutritional status of Methanosarcina acetivorans regulates glycogen metabolism and gluconeogenesis and glycolysis fluxes. *FEBS J* **283**:1979–1999.
- Shackelford DB and Shaw RJ (2009) The LKB1-AMPK pathway: metabolism and growth control in tumour suppression. *Nat Rev Cancer* **9**:563–575.
- Shaw RJ, Lamia KA, Vasquez D, Koo SH, Bardeesy N, Depinho RA, Montminy M, and Cantley LC (2005) The kinase LKB1 mediates glucose homeostasis in liver and therapeutic effects of metformin. *Science* **310**:1642–1646.
- Stone VM, Dhayal S, Smith DM, Lenaghan C, Brocklehurst KJ, and Morgan NG (2012) The cytoprotective effects of oleylethanolamide in insulin-secreting cells do not require activation of GPR119. *Br J Pharmacol* **165**:2758–2770.
- Suzuki T, Bridges D, Nakada D, Skiniotis G, Morrison SJ, Lin JD, Saltiel AR, and Inoki K (2013) Inhibition of AMPK catabolic action by GSK3. *Mol Cell* **50**:407–419.
- Viollet B (2017) The energy sensor AMPK: adaptations to exercise, nutritional and hormonal signals, in *Hormones, Metabolism and the Benefits of Exercise* (Spiegelman B ed) pp 13–24, Springer, Cham, Switzerland.
- von Wilamowitz-Moellendorf A, Hunter RW, Garcia-Rocha M, Kang L, López-Soldado I, Lantier L, Patel K, Peggie MW, Martínez-Pons C, Voss M, et al. (2013) Glucose-6-phosphate-mediated activation of liver glycogen synthase plays a key role in hepatic glycogen synthesis. *Diabetes* **62**:4070–4082.
- Woods A, Williams JR, Muckett PJ, Mayer FV, Liljevald M, Bohlooly-Y M, and Carling D (2017) Liver-specific activation of AMPK prevents steatosis on a high-fructose diet. *Cell Rep* **18**:3043–3051.
- Xu W, Zhou Q, Yin JJ, Yao Y, and Zhang JL (2015) Anti-diabetic effects of polysaccharides from *Talinum triangulare* in streptozotocin (STZ)-induced type 2 diabetic male mice. *Int J Biol Macromol* **72**:575–579.
- Yang X, Xu L, Zhou J, Ge Y, Wu S, Huang J, Li Y, Zhu M, Jin X, and Yang L (2019) Integration of phospholipid-complex nanocarrier assembly with endogenous n-oleylethanolamine for efficient stroke therapy. *J Nanobiotechnology* **17**:8.
- Yuan J, Tan JTM, Rajamani K, Solly EL, King EJ, Lecce L, Simpson PJJ, Lam YT, Jenkins AJ, Bursill CA, et al. (2019) Fenofibrate rescues diabetes-related impairment of ischemia-mediated angiogenesis by PPAR α -independent modulation of thioredoxin-interacting protein. *Diabetes* **68**:1040–1053.

Address correspondence to: Dr. Lichao Yang, School of Medicine, Xiamen University, Xiang'an District, Xiamen 361102, China. E-mail: yanglc116@xmu.edu.cn; or Enhui Yao, Department of Cardiology, Fujian Medical University Union Hospital, Fujian Institute of Coronary Artery Disease, Fujian Heart Medical Center, Fuzhou, China. E-mail: enhuiyao@hotmail.com

1 **Oleylethanolamide increases glycogen synthesis and inhibits hepatic**
2 **gluconeogenesis *via* the LKB1/AMPK pathway in type 2 diabetic model**

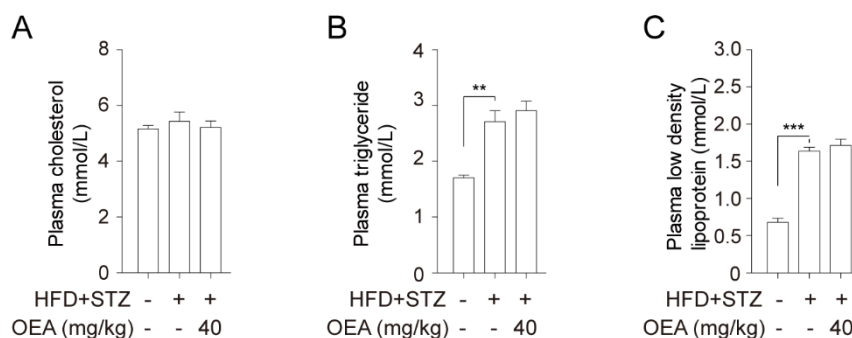
3 Tong Ren^a, Ang Ma^a, Rengong Zhuo^a, Huaying Zhang^a, Lu Peng^a, Xin Jin^a, Enhui
4 Yao^{b*}, Lichao Yang^{a*}

5



6 Supplemental Figure 1

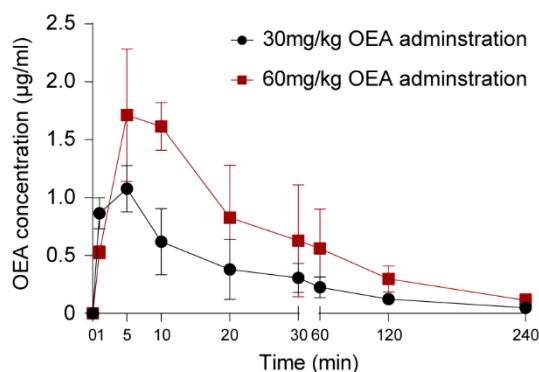
7 Supplementary Figure 1. The chemical structure of OEA and the schedule of animal
 8 experiments. (A) The chemical structure of OEA. (B) The schedule of animal
 9 experiments. Time points represent days after acclimation to living conditions. In
 10 experiment 1, animals were fed an HFD for 6 weeks (during days 1–42), and STZ was
 11 given on the 43rd day. OEA was subsequently administered for 6 weeks (during days
 12 44–86). In experiment 2, animals were fed an HFD for 6 weeks (during days 1–42), and
 13 STZ was given on the 43rd day. OEA was subsequently administered for 4 weeks
 14 (during days 44–72).



15 Supplemental Figure 2

16 Supplementary Figure 2. The effects of OEA on lipid profiles in diabetic PPAR α ^{-/-} mice.
 17 OEA-treated groups received single daily intraperitoneal injections of OEA (10, 30, 60
 18 or 40 mg/kg), and the normal and HFD+STZ groups were treated with vehicle on a
 19 daily basis. The levels of (A) total cholesterol, (B) total triglycerides and (C) low-

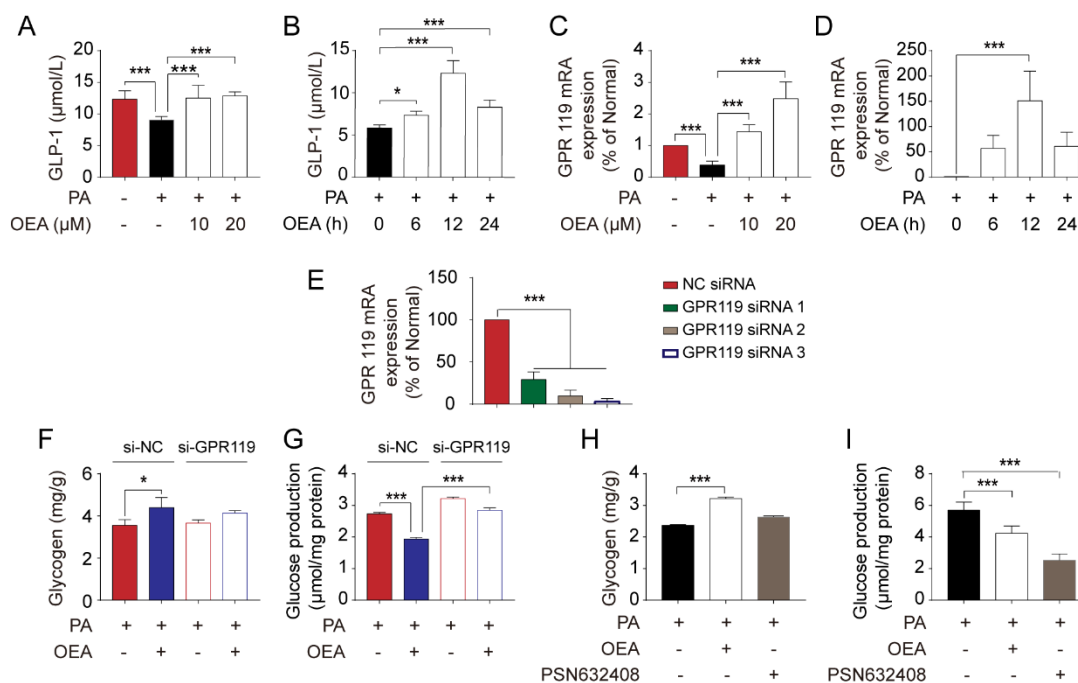
20 density lipoprotein. Values are means \pm S.E.M. (n=7 or 6 per group), * $P < 0.05$; ** $P <$
 21 0.01; *** $P < 0.001$.



22

Supplemental Figure 3

23 Supplementary Figure 3. OEA metabolism in serum and distribution in liver. Time
 24 course of OEA concentrations in plasma after *i.p.* administration in free-feeding rats.
 25 Values are means \pm S.E.M. (n=3-5 per group).

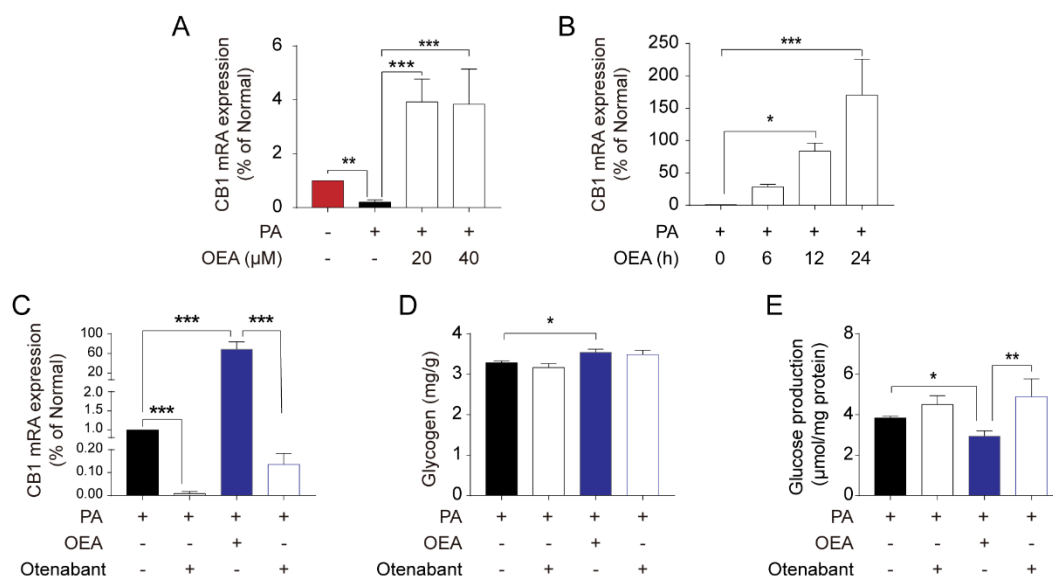


26

Supplemental Figure 4

27 Supplementary Figure 4. OEA reduced glycogen synthesis independent of GPR119
 28 pathway. OEA-treated cells received different concentrations of OEA (20 or 40 µM)
 29 for 24 h or 20 µM OEA for different times (6, 12 or 24 h), while the normal and PA-
 30 stimulated cells were treated with vehicle. (A and B) Quantitative analysis of GPR119

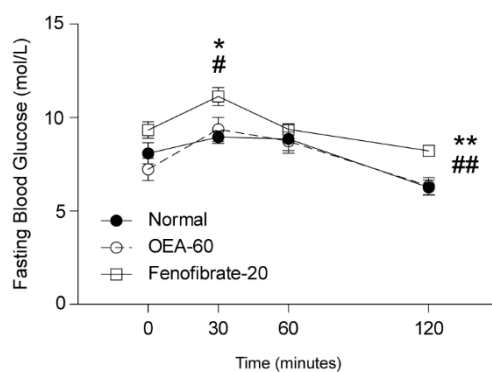
31 level. (C and D) Quantitative analysis of GPR119 mRNA expression. (F and H) The
 32 level of glycogen content. (G and I) The level of glucose production. The values are
 33 expressed as percentages compared to the normal or PA group and are represented as
 34 the means \pm S.E.M. of four separate experiments performed in duplicate ($n = 4$ per
 35 group), * $P < 0.05$; ** $P < 0.01$; *** $P < 0.001$.



36

Supplemental Figure 5

37 Supplementary Figure 5. OEA reduced glycogen synthesis independent of CB1
 38 pathway. OEA-treated cells received different concentrations of OEA (20 or 40 μ M)
 39 for 24 h or 20 μ M OEA for different times (6, 12 or 24h), while the normal cells were
 40 treated with vehicle. (A and B) Quantitative analysis of CB1 mRNA expression.
 41 Primary hepatocytes were subjected to the CB1 inhibitor otenabant for 12 h, followed
 42 by OEA (20 μ M) treatment for an additional 12 h. (C) Quantitative analysis of GPR119
 43 mRNA expression. (D and E) The levels of glycogen content and glucose production.
 44 The values are expressed as percentages compared to normal or PA group and are
 45 represented as the means \pm S.E.M. of five separate experiments performed in duplicate
 46 ($n = 4$ per group), * $P < 0.05$; ** $P < 0.01$; *** $P < 0.001$.

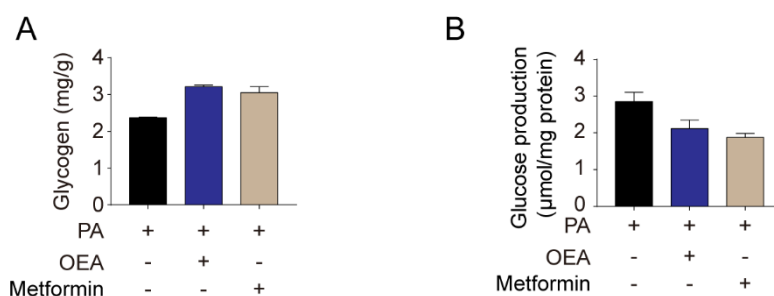


Supplemental Figure 6

47

48 Supplementary Figure 6. Effects of OEA on glucose tolerance in normal KM mice. The
 49 OEA-treated group received single daily intraperitoneal injections of OEA (60 mg/kg),
 50 and the Fenofibrate-treated group received single daily oral treatments of fenofibrate
 51 (20 mg/kg). The normal groups were treated with vehicle on a daily basis. OGTT assay
 52 was performed after 15 weeks of treatment. Values are means \pm S.E.M. (n=10 per
 53 group). $^{\#}P < 0.05$ vs. the normal group; $^{\#\#}P < 0.01$ vs. the normal group; $^*P < 0.05$ vs.
 54 the HFD+ STZ group; $^{**}P < 0.01$ vs. the HFD+STZ group.

55



Supplemental Figure 7

56

57 Supplementary Figure 7. Effect of OEA and metformin on glycometabolism in PA-
 58 stimulated mouse primary hepatocytes. Mouse primary hepatocytes received 20 μ M
 59 OEA and 20 μ M metformin for 12 h. The levels of (A) glycogen content and (B)
 60 glucose production. The values are represented as the means \pm S.E.M. of five separate
 61 experiments performed in duplicate (n = 4 per group), $^{**}P < 0.01$.